Journal of Molecular Catalysis A: Chemical 367 (2013) 7–11

Contents lists available at SciVerse ScienceDirect

Journal of Molecular Catalysis A: Chemical

journal homepage: www.elsevier.com/locate/molcata

Immobilization of cobalt porphyrin on $CeO_2@SiO_2$ core–shell nanoparticles as a novel catalyst for selective oxidation of diphenylmethane

Xiang Guo, Yuan-Yuan Li, Dan-Hua Shen, Yuan-Yuan Song, Xiao Wang, Zhi-Gang Liu*

School of Chemistry and Chemical Engineering, Hunan University, Changsha, Hunan 410082, PR China

ARTICLE INFO

Article history:
Received 13 August 2011
Received in revised form 30 May 2012
Accepted 1 November 2012
Available online 16 November 2012

Keywords:
Core–shell
Cobalt porphyrin
Ceria
Diphenylmethane
Selective oxidation

ABSTRACT

In this study, $CeO_2@SiO_2$ core–shell nanoparticles have been synthesized and used as supports to graft cobalt porphyrin via an amide bond. The catalyst was characterized using techniques such as FT-IR, UV–vis, SEM, TEM and BET. The results show that the catalyst was composed of regular nanoparticles (around 50 nm) with a core–shell structure. In addition, the catalyst exhibits an excellent activity, selectivity and stability for solvent-free selective oxidation of diphenylmethane with atmospheric pressure of oxygen. The conversion of diphenylmethane was as high as 41.6% with selectivity to diphenyl ketone of 96.3%. Even after reused up to 6 times, the catalyst maintained stable working ability.

1. Introduction

Supported metalloporphyrin catalysts have been used as effective catalysts for a wide range of selective oxidations of hydrocarbons, for the micro-environment of the support can bring higher selectivity and prevent catalyst self-oxidation [1,2]. Therefore, there has been a wide-spread interest in the synthesis of metalloporphyrin catalysts supported on inorganic, organic, or hybrid materials, especially those with a core–shell structure [3–6].

Because of the advantages of core–shell structured nanocomposites resulting in non-aggregated nanoparticles with a controlled surface and/or coating properties [7–10], the prospect of materials with core–shell structure used as catalyst carriers has attracted more attention. Huang et al. [11,12] employed magnetic polymer nanospheres (with Fe_3O_4 core and polystyrene shell) as a support of metalloporphyrin. It was found that these nanospheres have good magnetic responsiveness and thus can be recycled by employing an external magnetic field. Liu et al. [13] adopted silica-coated Fe_3O_4 nanoparticles as a carrier and synthesized a series of supported metalloporphyrin catalysts with different saturation magnetization. The influence of the saturation magnetization of magnetic Fe_3O_4 nanoparticles on the catalytic abilities of supported metalloporphyrin was also investigated. Unfortunately, the effect of Fe_3O_4 embedded in the nanospheres on catalysis of the nanospheres was reported to be negligible and cannot be used as promoter of catalysts [12].

CeO_2 is a well-known promoter additive because of its oxygen storage and releasing capacity [14,15]. Herein, CeO_2 was expected to be used as the core in the core–shell materials since CeO_2 possesses catalytic activity and cooperates with metalloporphyrin in redox reactions.

However, the surface precipitation of ceria on silica is inadequate when precipitant such as ammonium solution is used [16], because the pH of the precipitate is 10, surface of silica is negatively charged, and the pH of ceria is above 8. As a result, silica could not coat the ceria as core due to the expected electrostatic repulsion between both particles. To induce the attraction interaction between the silica and ceria, Grasset et al. [17] moved the pH of the silica–ceria suspension to pH 4, where the silica and ceria were oppositely charged with respect to each other.

However, it could not look forward to lower the pH with the addition of acid when ammonium solution was used as precipitant during the synthesis of $CeO_2@SiO_2$. To achieve the electrostatic attraction between the silica–ceria, the surface of the silica particles was modified with amine group via the hydrolysis of 3-aminopropyl-trieth-oxysilane [18].

As illustrated in Scheme 1, we used citrate sodium to modify the surface properties of ceria and synthesized the $CeO_2@SiO_2$ core–shell structured support. Cobalt porphyrin was then immobilized on these synthesized $CeO_2@SiO_2$ structures for the first time. The catalysts were characterized using FT-IR, UV–vis, SEM, TEM, XRD and BET, and the catalytic performance for solvent-free oxidation of diphenylmethane to diphenyl ketone was measured. The

---

* Corresponding author. Tel.: +86 731 88821314; fax: +86 731 88821667.
E-mail addresses: liuzhigang@hnu.edu.cn, cerialiu@gmail.com (Z.-G. Liu).

1381-1169/$ – see front matter © 2012 Elsevier B.V. All rights reserved.
http://dx.doi.org/10.1016/j.molcata.2012.11.005

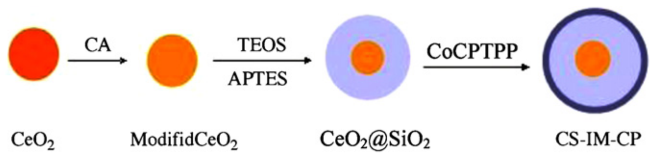

Scheme 1. Illustration of the major steps for preparation of CoCPTPP grafted on $CeO_2@SiO_2$ nanoparticles.

results show that the catalysts exhibit excellent catalytic activity, selectivity and stability.

2. Experimental

2.1. Materials

5-(4-Carboxyphenyl)-10,15,20-triphenyl porphyrin (CPTPP) was synthesized and purified in our laboratory. The metal oxides used in this work were prepared with coprecipitation method from corresponding metal nitrates. Water used in all experiments was deionized and doubly distilled prior to use. 4-Carboxy benzaldehyde, benzaldehyde and pyrrole were redistilled before use. All other reagents were obtained commercially and used without further purification.

2.2. Characterization of catalysts

UV–vis patterns were recorded on a Shimadzu UV-2450 spectrophotometer using $BaSO_4$ as reference with a range of 200–800 nm and a scan step of 0.5 nm. FT-IR spectra were measured on an Agilent Perkin-Elmer 783 infrared spectrometer in KBr disc. The specific surface areas of samples were determined by analyzing the results of N_2 adsorption at −196 °C in a Micromeritics ASAP 2020 apparatus and applying the Brunaumer–Emmett–Teller (BET) method to the experimental values. All samples were dehydrated at 150 °C for 24 h prior to N_2 adsorption. SEM (JSM 6700F) was used to observe the particle sizes and shapes of samples. Prior to the measurements, the samples were mounted on a carrier made from glassy carbon and coated with a film of gold. TEM (Hitachi 800, operated at 175 kV) images were obtained by dispersing samples in ethanol using an ultrasonication bath and then depositing a drop of liquid containing the particles onto a copper grid.

2.3. Synthesis of catalysts

2.3.1. Synthesis of cobalt(II) 5-(4-carboxyphenyl)-10,15,20-triphenyl porphyrin

According to literature [19], 200 mL of propanoic acid, 0.0525 mol of benzaldehyde and 0.0175 mol of 4-carboxy benzaldehyde were loaded into a three-neck flask and heated to reflux under stirring, then 0.07 mol of pyrrole was slowly dropped through a funnel within 20 min. Under refluxing condition, the mixture was stirred for 30 min. After cooling the reaction solution in a refrigerator overnight the mixture was then filtered and purified by column chromatography and 5-(4-carboxyphenyl)-10,15,20-triphenyl porphyrin was obtained. 0.50 g of obtained porphyrin was dissolved in 100 mL of N,N-dimethylformamide (DMF), and 2.54 g of $CoCl_2{\cdot}6H_2O$ was added under stirring, and then heated to reflux until porphyrin detected by TLC was exhausted. After cooling overnight, this mixture was filtered and washed repeatedly with hot water, cobalt(II) 5-(4-carboxyphenyl)-10,15,20-triphenyl porphyrin (CoCPTPP) was achieved.

2.3.2. Synthesis of surface modified CeO_2

Surface modified CeO_2 was synthesized according to literature methods [20,21]. 5.996 g of $Ce(NO_3)_3{\cdot}6H_2O$ was added into volumetric flask and prepared for 250 mL of solution with deionized water. Under mechanical stirring, 250 mL 0.36 M of NaOH solution was slowly dropped into $Ce(NO_3)_3$ solution until the solution pH was 13. After stirring for 30 min, the precipitate was filtered and washed with deionized water twice and then dispersed in 200 mL 0.3 M of citrate sodium solution. After stirring at 90 °C for 6 h, the product was filtered, washed with ethanol and water, respectively, and dried. The modified CeO_2 was achieved.

2.3.3. Synthesis of $CeO_2@SiO_2$ with core–shell structure

$CeO_2@SiO_2$ nanoparticles were prepared as described in the literature [22,23]. Namely, 0.30 g of CeO_2 was well dispersed in the mixture of ethanol (160 mL), deionized water (40 mL) and concentrated ammonia aqueous solution (5.0 mL, 28 wt.%), followed by addition of tetraethyl orthosilicate (TEOS, 1 mL) and 3-aminopropyltriethoxysilane (APTES, 0.2 mL). After stirring for 6 h at room temperature, the product was filtered and washed with ethanol and water. The obtained $CeO_2@SiO_2$ core–shell nanoparticles were denoted as CS, with the specific surface area 50.8 m^2/g. Nanoparticles without coating CeO_2 were synthesized by the similar method and denoted as NCS.

2.3.4. Synthesis of CoCPTPP anchored on $CeO_2@SiO_2$

According to literature [24], 0.05 g of CoCPTPP, 3.50 g of CS and 150 mL N,N-dimethylformamide (DMF) were loaded into a three-neck flask, then heated to reflux for 12 h. After cooling, washing with deionized water and filtering, dichloromethane was used to extract the sample in a Soxhlet extractor till the extracted solution was turned to clarify. The product was designated as CS-IM-CP. The specific surface area of CS-IM-CP was 25.9 m^2/g and CoCPTPP loading in CS-IM-CP was 7.9 mg/g-cat. Following the similar procedure, CoCPTPP was immobilized on NCS, and the product was denoted as CS-IM-CP with CoCPTPP loading of 8.2 mg/g. The CoCPTPP loading in CS-IM-CP was determined by UV–vis quantitative analysis method.

2.4. Measurement of catalytic performance

The catalytic performance of catalysts for solvent-free oxidation of diphenylmethane was measured in a 100 mL four-neck flask with a magnetic stirrer. In a typical experiment, 30 mL of diphenylmethane and 100 mg of catalyst were loaded into the glass reactor. The reactor was sealed and bubbled with oxygen at atmospheric pressure. The reactor was then heated to desired reaction temperature in an oil bath under stirring. Every hour, 0.5 mL of samples were withdrawn with a syringe and analyzed by gas chromatography with internal standard method using chlorobenzene as reference substance. After the reaction, the reactor was cooled to room temperature and the product was filtered through a millipore filter. Then, the catalyst was recovered and dried at 80 °C for 12 h. The regenerated catalyst was used for cycling studies.

3. Results and discussion

3.1. Characterization of catalysts

Solid-state diffuse-reflectance UV–vis spectroscopy was typically used to analyze metalloporphyrin species because metalloporphyrin species have characteristic peaks, called as Soret band and Q-band, respectively [25]. In Fig. 1, the characteristic bands of CS-IM-CP in the UV–vis spectra can be found at 428 nm and 541 nm. The support CS was measured by UV–vis spectra without characteristic peaks. As for CS-IM-CP, the characteristic peaks of

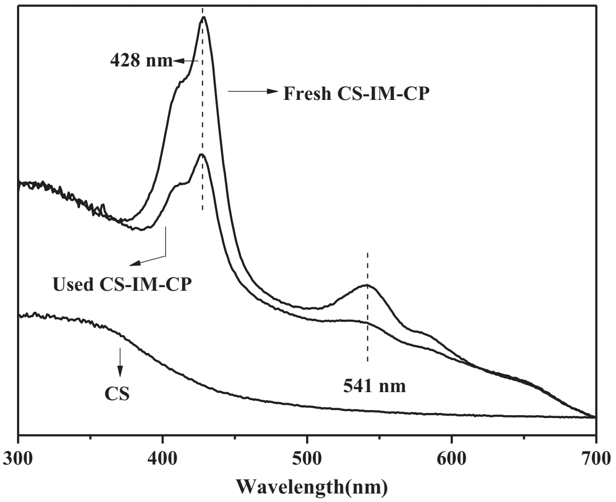

Fig. 1. UV–vis spectra of CS-IM-CP and CS.

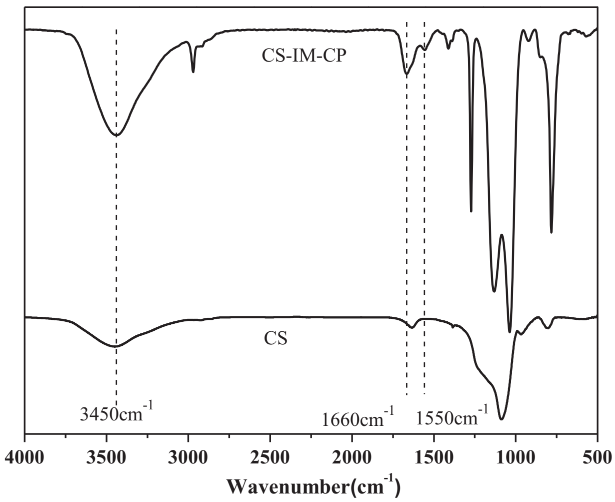

Fig. 2. FT-IR spectra of catalysts (CS and CS-IM-CP).

cobalt porphyrin were expected to appear at 428 nm and 541 nm, respectively. Because no peaks were seen in the CS spectrum, the peaks at 428 nm and 541 nm must be the synthesized cobalt porphyrin supported on CS. In addition, CS-IM-CP was extracted with dichloromethane in a Soxhlet extractor until the extracted solution was turned to clarify. This indicates that no physical absorption cobalt porphyrin existed in CS-IM-CP. Therefore, we can confirm that that cobalt porphyrin has been immobilized via covalent bond on the silica surface.

Many kinds of covalent bonds such as C—O—C, C—N and N—C═O can be employed to anchor cobalt porphyrin on the surface of supports [13,26,27]. In this study, N—C═O was formed via dehydrolysis reaction among the precursors with functional groups of COOH and NH_2. In Fig. 2 the FTIR spectra of CS-IM-CP is shown. The absorption bands observed at 1040–1260 cm^{-1} were ascribed to stretching vibrations of Si—O—Si and O—H in silanols. The absorption bands which appeared at 1690–1630 cm^{-1} due to the C═O group in amide (N—C═O) demonstrate that the cobalt porphyrin was covalently bound to the silica support. In addition, both CS and CS-IM-CP have the characteristic absorption of the N—H group observed near 1550 cm^{-1}. However, It verified that CoCPTPP has been immobilized in CS through an amide bond. The peak of the N—H group in CS-IM-CP, compared with CS, has a blue shift, which was assumed to the influence of C═O group in amide [26].

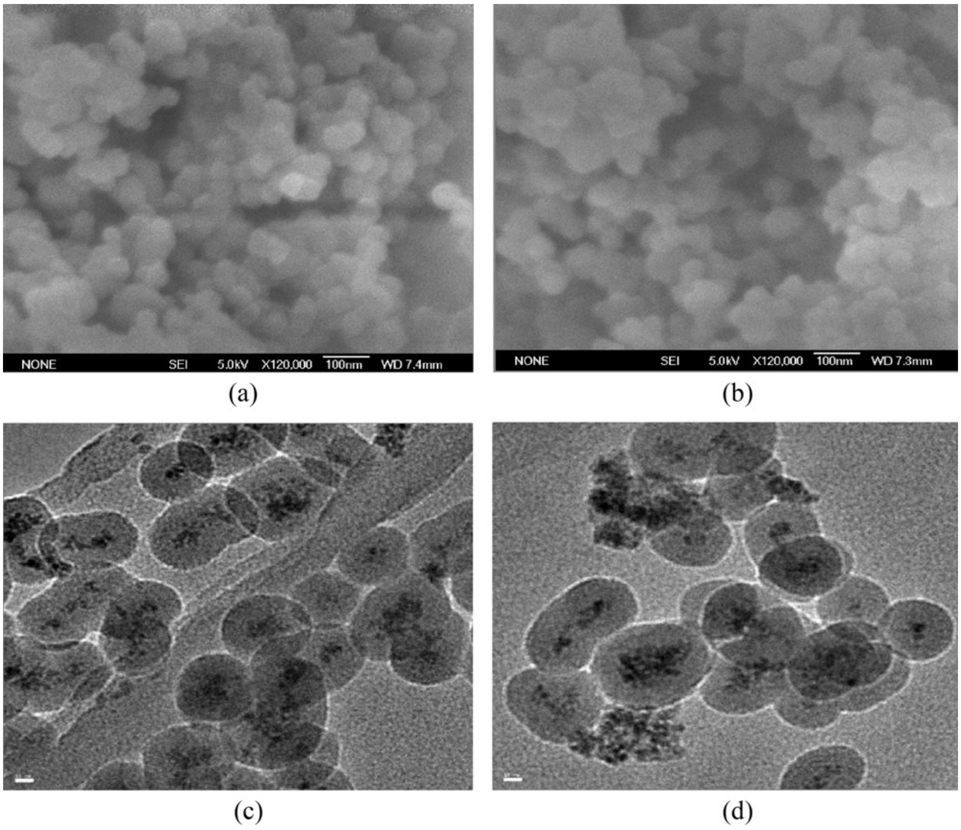

(a) (b)

(c) (d)

Fig. 3. SEM patterns of catalysts (a) CS and (b) CS-IM-CP, TEM patterns of catalysts (c) CS and (d) CS-IM-CP.

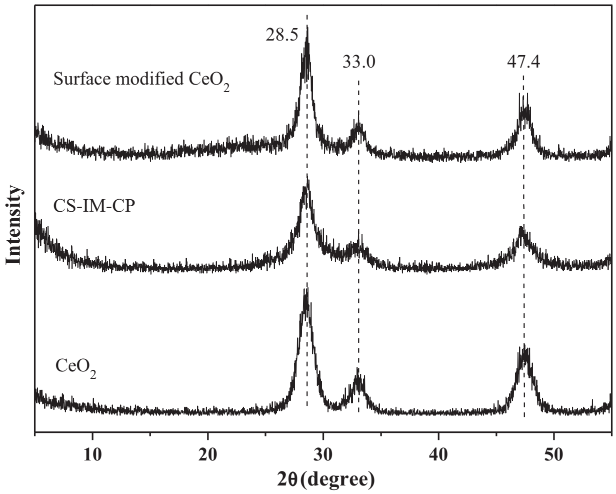

Fig. 4. Wide-angle XRD patterns of CeO_2, surface modified CeO_2 and CS-IM-CP.

It indicates cobalt porphyrin was anchored on the surface of silica via amide.

SEM micrographs of CS and CS-IM-CP are presented in Fig. 3(a) and (b). In both cases the nanoparticles consisted of an arrangement of relatively uniform particles with a particle size of around 50 nm. This means the morphology of $CeO_2@SiO_2$ has changed little during the immobilization of CoCPTPP. Fig. 3(c) and (d) displays TEM micrographs of samples, respectively. The presence of $CeO_2@SiO_2$ core–shell nanoparticles is clearly shown and the CeO_2 can easily be seen at the center of the structure. However, the aggregation of CeO_2 nanoparticles was observed and seemed to be dispersed beside $CeO_2@SiO_2$ core–shell nanoparticles. Typically, the concentration of CeO_2 is 25% in the $CeO_2@SiO_2$ core–shell nanoparticles or even lower as reported in other studies [16,17]. Here, the concentration of CeO_2 in the $CeO_2@SiO_2$ core–shell nanoparticles is 53%, much larger than 25%. The overloading may be the cause of the appearance of bulk CeO_2 nanoparticles.

In Fig. 4, it can be seen that the distinct diffraction peaks of CeO_2 were observed at 28.5, 33.0 and 47.4, respectively [28]. This result indicates that the CeO_2 in $CeO_2@SiO_2$ composite particles is in cubic flourite structure. No peaks of SiO_2 were observed in the pattern of $CeO_2@SiO_2$ composite particles, which may be due to the fact that the as-prepared SiO_2 particles exist as an amorphous phase at this temperature [18]. In addition, no new phases were detected, which demonstrate that CeO_2 and SiO_2 are independent phases in the composite particles.

3.2. Solvent-free oxidation of diphenylmethane by dioxygen at ambient pressure

Diphenylmethanone is a very important feed stock used in fragrance, as an initiator and so on. Here we consider the reaction of diphenylmethane to diphenylmethanone as the model reaction. Molecular oxygen was used as an oxidant and the reaction pressure was kept at ambient pressure. The catalytic performance of the catalysts for oxidation of diphenylmethane is shown in Table 1. Compared with CS-IM-CP and CoCPTPP, CeO_2 and CS have lower conversion (15.6% and 17.0%) with a similar selectivity. When metalloporphyrin was immobilized on the surface of CS, the diphenylmethane conversion over CS-IM-CP reaches 41.6%. This result means that the catalytic activity of catalysts is remarkably improved after the immobilization of CoCPTPP. In addition, the conversion of NCS-IM-CP is lower than that of CS-IM-CP by 4.3%, which agrees with our previous studies [24] showing that ceria can act as a promoter, cooperating with metalloporphyrins and enhancing the activity of CS-IM-CP.

Table 1
Selective oxidation of diphenylmethane to diphenyl ketone.[a]

Catalyst	Time (h)	Conversion (%)	Diphenyl ketone selectivity (%)
CeO_2	24	17.0	97.0
CS	24	15.6	97.8
CS-IM-CP	24	41.6	96.3
NCS-IM-CP	24	37.3	96.1

[a] Reaction condition: catalyst: 100 mg; diphenylmethane: 30 mL; flow of O_2: 200 mL/min; temperature: 130 °C; pressure: 1 atm; reaction time: 24 h.

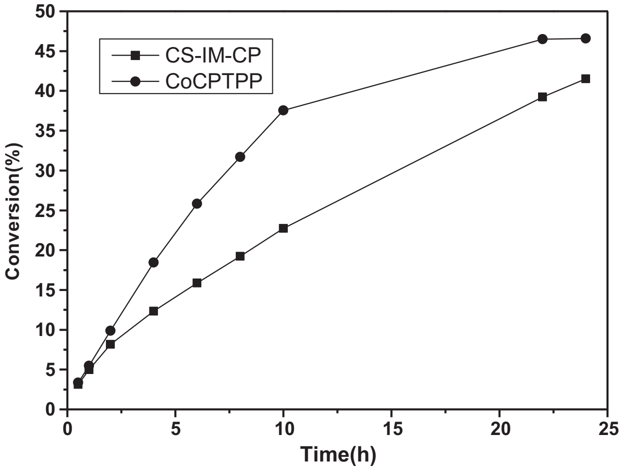

Fig. 5. Influence of reaction time for oxidation of diphenylmethane over CS-IM-CP and CoCPTPP; reaction condition: catalyst: 100 mg; diphenylmethane: 30 mL; flow of O_2: 200 mL/min; temperature: 130 °C; pressure: 1 atm; reaction time: 24 h.

The stability of CS-IM-CP for oxidation of diphenylmethane is shown in Fig. 5. In Fig. 5, the conversion of diphenylmethane over CoCPTPP is a little higher than that of CS-IM-CP in 24 h. This can be explained by the fact that the active center can more easily interact with the substrate in the monophase. Alternatively, when immobilized on $CeO_2@SiO_2$, the stability of CoCPTPP is evidently improved and has a high reusability, though the activity of CS-IM-CP may be a little lower than that of CoCPTPP.

Fig. 6 demonstrates the reusability of CS-IM-CP for oxidation of diphenylmethane. After the reaction CS-IM-CP was recycled by simple filtration of the catalyst, the solid remnants with MeOH

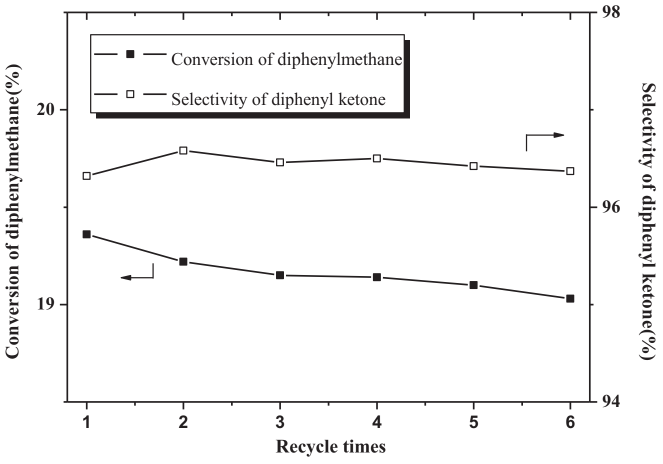

Fig. 6. Stability of CS-IM-CP for selective oxidation of cyclohexane. Reaction condition: catalyst: 100 mg; diphenylmethane: 30 mL; flow of O_2: 200 mL/min; temperature: 130 °C; pressure: 1 atm; reaction time: 8 h.

were washed off and dried at 80 °C for 12 h. Diphenylmethane and oxygen were then introduced to the catalytic material and the catalyzed reaction restarted. In Fig. 6, it can be clearly observed that CS-IM-CP, which was reused up to six times, only slightly decreases and shows high stabilization. In fact, supported metalloporphyrin deactivation is a very common occurrence in oxidation reactions of alkane [12,13]. In these systems, the deactivation was believed to be a result of decomplexation of the metalloporphyrin bound to the silica support. The precursor to the decomplexation is a μ-oxo-bridged dimer which is also inactive in diphenylmethane catalysis.

Meanwhile, the UV–vis spectra of the used catalyst demonstrate the characteristic peaks of cobalt porphyrin ring and is almost the same as that of the fresh one. This indicates the structure of porphyrin ring still exists. Furthermore, no new peaks appear which indicates no presence of new species. It also disagrees with the opinion of the formation of a μ-oxo-bridged dimer [27]. However, the intensity of the peaks of the used catalyst was lowered than that of the fresh one. It can be explained by some leaching or decomposing of the cobalt porphyrin grafted on the CS which happened during the reaction. All in all, though the supported cobalt porphyrin may suffer from the leaching and decomposing during the reaction, CS-IM-CP has a higher stability and reusability than their encounter homogeneous cobalt porphyrin.

4. Conclusions

CoCPTPP immobilized on $CeO_2@SiO_2$, i.e., CS-IM-CP, can be synthesized by amidation reaction, bearing core–shell structures with satisfying morphology. The catalyst shows excellent catalytic activity, selectivity and stability for solvent-free highly selective oxidation of diphenylmethane by oxygen at ambient pressure. The conversion of diphenylmethane over CS-IM-CP is 41.6% and the selectivity to diphenyl ketone is 96.3% when the reaction is running for 24 h. Moreover, these catalysts, which can be effectively and effortlessly recovered, can retain their high catalytic activities after being recycled six times.

Acknowledgment

The authors gratefully acknowledge the financial support from Hunan Province Natural Science Foundation of China (No. 10JJ4008).

References

[1] A.F. Trindade, M.P. Gois, A.M. Afonso, Chem. Rev. 109 (2009) 418–514.
[2] N.E. Leadbeater, M. Marco, Chem. Rev. 102 (2002) 3217–3274.
[3] B.J. Gao, R.X. Wang, Y. Zhang, J. Appl. Polym. Sci. 112 (2009) 2764–2772.
[4] G.S. Machado, F. Wypych, S. Nakagaki, et al., J. Catal. 274 (2010) 130–141.
[5] M. Moghadam, S. Tangestaninejada, V. Mirkhania, et al., J. Mol. Catal. A: Chem. 337 (2011) 95–101.
[6] Y.J. Ye, J.W. Huang, L.N. Ji, et al., J. Mol. Catal. A: Chem. 331 (2010) 29–34.
[7] S.H. Hu, X.H. Gao, J. Am. Chem. Soc. 132 (2010) 7234–7237.
[8] C. Cannas, A. Musinu, A. Ardu, et al., Chem. Mater. 22 (2010) 3353–3361.
[9] S.K. Basiruddin, A. Saha, N.R. Jana, J. Phys. Chem. C 114 (2010) 11009–11017.
[10] V. Ervithayasuporn, Y. Kawakami, J. Colloid Interface Sci. 332 (2009) 389–393.
[11] B. Fu, H.C. Yu, J.W. Huang, P. Zhao, J. Liu, L.N. Ji, J. Mol. Catal. A: Chem. 298 (2009) 74–80.
[12] B. Fu, P. Zhao, H.C. Yu, J.W. Huang, J. Liu, L.N. Ji, Catal. Lett. 127 (2009) 411–418.
[13] C.X. Liu, Q. Liu, C.C. Guo, Catal. Lett. 138 (2010) 96–103.
[14] M.P. Woods, P. Gawade, B. Tan, U.S. Ozkan, Appl. Catal. B: Environ. 97 (2010) 28–35.
[15] M.M. Natile, A. Glisenti, Chem. Mater. 17 (2005) 3403–3414.
[16] T. Tago, S. Tashiro, Y. Hashimoto, K. Wakabayashi, M. Kishida, J. Nanopart. Res. 5 (2003) 55–60.
[17] F. Grasset, R. Marchand, A.M. Maric, D. Fauchadour, F. Fajardie, J. Colloid Interface Sci. 299 (2006) 726–732.
[18] X.B. Zhao, R.W. Long, Y. Chen, Z.G. Chen, Microelectron. Eng. 87 (2010) 1716–1720.
[19] C.B. Hansen, G.J. Hoogers, W. Drenth, J. Mol. Catal. A: Chem. 79 (1993) 153–163.
[20] Z.G. Liu, R.X. Zhou, X.M. Zheng, J. Mol. Catal. A: Chem. 255 (2006) 103–138.
[21] T. Aubert, F. Grasset, E. Duguet, et al., J. Colloid Interface Sci. 341 (2010) 201–208.
[22] W. Stöber, A. Fink, E.J. Bohn, J. Colloid Interface Sci. 26 (1968) 62–69.
[23] X.Q. Xu, C.H. Deng, X.M. Zhang, et al., Adv. Mater. 18 (2006) 3289–3293.
[24] Z.G. Liu, X. Guo, Y.Y. Li, et al., Appl. Catal. A: Gen. 413–414 (2012) 30–35.
[25] G. Huang, T.M. Li, S.Y. Liu, et al., Appl. Catal. A: Gen. 371 (2009) 161–165.
[26] K.A.D.F. Castro, A. Bail, P.B. Groszewicz, G.S. Machado, W.H. Schreiner, F. Wypych, S. Nakagaki, Appl. Catal. A: Gen. 386 (2010) 51–59.
[27] A.R. McDonald, N. Franssen, G.P.M. Klink, G. Koten, J. Organomet. Chem. 694 (2009) 2153–2162.
[28] Z.G. Liu, R.X. Zhou, X.M. Zheng, J. Mol. Catal. A: Chem. 267 (2007) 137–142.